JOURNAL OF GEOPHYSICAL RESEARCH, VOL. 104, NO. C4, PAGES 7921–7933, APRIL 15, 1999

Estimation of salinity profiles in the upper ocean

Donald V. Hansen

Cooperative Institute for Marine and Atmospheric Studies, University of Miami, Miami, Florida

W. Carlisle Thacker

Atlantic Oceanographic and Meteorological Laboratory, National Oceanic and Atmospheric Administration, Miami, Florida

Abstract. A new algorithm is presented for estimating salinity profiles in the upper ocean from measurements of temperature profiles and surface salinity. In application to the eastern tropical Pacific the method replicates a large fraction of the variability of salinity in the upper few tens of meters and provides modest to substantial improvement at nearly all levels. Estimated salinity profiles are able to characterize barrier layers, regions formed by a halocline within the thermal mixed layer. The rms error of geopotential height calculations based on estimated salinity profiles is reduced more than 50% by this method relative to methods not using surface salinity. Even without the surface salinity measurement some reduction of error in geopotential heights can be obtained relative to previous methods.

1. Introduction

Salinity and temperature profiles have been used historically for characterizing ecosystems and for calculating ocean currents by the geostrophic method. Oceanic analyses based on assimilation of observations into ocean circulation models [*Ji and Leetmaa*, 1997] for forecasting climate can serve these needs as well. Recent emphasis has been on assimilation of measurements of sea-surface temperature from ships, buoys, and satellites, and upper ocean temperature-profile measurements from expendable bathythermographs (XBTs) and buoys. Because sea-surface temperature is the most important air-sea interaction variable and subsurface temperature the dominant variable for determination of sound speed, the technology for economical measurements have been developed only for temperature. Thus thousands of temperature profiles are being collected in the upper ocean and used in analyses. However, density or specific volume is the important dynamic variable in the ocean, and density is determined by both temperature and salinity.

Acero-Shertzer et al. [1997] discovered discrepancies in surface currents from the National Centers for Environmental Prediction's oceanic analyses that were attributed to deficiencies in the treatment of salinity. Salinity was initialized with climatological values but was not controlled subsequently by either fluxes or assimilation of observations. The discrepancy most easily quantified is the influence of salinity on geopotential height of the sea surface. Salinity rapidly homogenized in the model, which with assimilation of temperature observations resulted in a transequatorial difference in mean geopotential height anomaly of 25 to 30 cm in the central Pacific Ocean, approximately double the climatological mean value. The excessive geopotential height gradient forced excessive current speeds in the North Equatorial Countercurrent and especially the South Equatorial Current in the western Pacific. This result, including the implication that some model fields could be degraded by assimilation of temperature but not salinity, was anticipated by *Cooper* [1988].

Carton and Hackert [1990] recognized the tendency for homogenization and avoided its effects by taking seasonal climatological fields for their salinity analyses. This strategy precludes modeling salinity fluxes or effects of salinity anomalies. In some regions it can be a source of substantial error. In model studies *Reason* [1992] found that rainfall variability can result in surface currents that differ from their climatological values by 10% to as much as 100%. *Emery and Dewar* [1982] found that rms errors in geopotential height of the sea surface relative to 500 dbar of order 10 cm can accrue from use of mean salinity in lieu of measured profiles. They also found that by use of a regional temperature-salinity relationship as proposed by *Stommel* [1947], the rms errors can be reduced but only to something less than 8 cm. In latitudes higher than about 35°N in the North Pacific, they found the mean salinity to serve better.

The other discrepancy identified by *Acero-Shertzer et al.* [1997], excessive divergence of equatorial surface currents, was attributed to insufficient downward mixing of momentum from surface wind stress. This discrepancy in the model may be due partly to the mixing algorithms used [*Schneider and Müller*, 1994], partly to the value of empirical constants used with them, and partly to inaccurate representation of the density stratification that is required in the algorithms.

Poorly modeled salinity can lead to a poor representation of density stratification. *Reynolds et al.* [1998] have documented the need for more salinity profiles for oceanic analyses.

Lucas and Lindstrom [1991] recently called attention to the frequent occurrence in the western tropical Pacific Ocean of a halocline within the near-surface thermal mixed layer, which restricts the thickness of the upper ocean participating in air-sea interactions. *Roemmich et al.* [1994] suggested that horizontal gradients of salinity in the surface mixed layer contribute to formation of these restrictive "barrier layers."

Much of the recent interest in the effects of salinity has concerned the dynamics and thermodynamics of the upper ocean. Improved modeling of salinity also opens the possibility of other applications. The success of *Delcroix et al.* [1996] in demonstrating at least semiquantitative relationships between sea-surface salinity and precipitation over the tropical Pacific Ocean suggests use of ocean analyses for estimating precipitation and evaporation. This application is particularly attractive for use in tropical regions where understanding and prediction of seasonal-to-interannual variations like the El Niño – Southern Oscillation (ENSO) and regional precipitation are major objectives. Improved modeling of the vertical structure of both salinity and currents in the upper ocean should be of value also for questions of longer term climate variations, such as the meridional transport of fresh water in the North Atlantic Ocean, which is understood to be an important factor in formation of North Atlantic Deep Water, which in turn is responsible for the large poleward heat flux in the North Atlantic [*Rahmstorf*, 1996; *Wijffels et al.*, 1992].

In this paper we present a new strategy to estimate salinity profiles for assimilation into numerical circulation models or for such other applications as they may be needed. The main objective is estimation of salinity profiles in the upper ocean from measurements of temperature profiles and surface salinity. The latter can be made inexpensively from volunteer observing ships [*Hénin and Grelet*, 1996] where they are available, from surface buoys elsewhere, and potentially by remote sensing [*Lagerloef et al.*, 1995; *Miller et al.*, 1998]. A secondary result is an algorithm for more accurate estimation of salinity profiles from temperature profiles even without the additional measurement of surface salinity.

The most frequently used method for estimating salinity has been the climatological average. Numerical models of oceanic circulation are usually initialized in this way [*Chassignet et al.*, 1996; *Ji et al.*, 1995], and this approach has also been used for updating model runs in which other variables are being assimilated from observations [*Carton and Hackert*, 1990]. Although this procedure suppresses the effects of salinity anomalies, the results of *Sprintall and Tomczak* [1992] indicate that it can capture at least part of the barrier layer phenomenon.

Stommel [1947] proposed use of the statistical relationship between salinity and temperature (*T-S*) to estimate salinity from more plentiful temperature-profile data: $\hat{S}(z) = \bar{S}[T(z)]$. (An overbar is used to indicate average at fixed temperature, while angular brackets will be used to indicate average at fixed depth. $\hat{S}(z)$ denotes the estimated value for salinity at the depth z.) This method has found use in regions having a well-defined temperature-salinity (*T-S*) relation, i.e., in regions of sufficiently uniform water mass characteristics. *Flierl* [1978] devised a modification of the method whereby a small number of observed salinity profiles can be used to determine a local rule for estimating salinity profiles from temperature profiles in frontal zones of contrasting water masses. This modification is not suitable for application to the diverse conditions usually observed in near-surface waters. *Donguy et al.* [1986] introduced another modification of the basic method for a data set in which temperature profiles were complemented by measurements of surface salinity. They estimated salinity from a *T-S* relationship for which the near-surface portion is defined by linear interpolation from monthly average surface salinity and temperature to the subsurface salinity maximum that is characteristic of much of the tropical Pacific. *Kessler and Taft* [1987] similarly interpolated linearly from the surface observation to a subjectively chosen level below which a well-defined *T-S* relationship could be found. *Stommel's* [1947] method in any of its variations can replicate salinity anomalies that are correlated with temperature anomalies; it cannot produce barrier-layer structures that violate the assumption that salinity and temperature have the same functional dependence on depth.

Vossepoel et al. [1999] have recently introduced a hybrid scheme that estimates salinity below the bottom of the thermally mixed layer by the *T-S* method and within the isothermal layer by linear interpolation to a measured sea-surface salinity. This method frequently will yield fictitious barrier layers beginning right at the surface in tropical regions. Where surface salinity is anomalously high it also can produce fictitious density inversions beginning at the surface. *Vossepoel et al.* [1999] propose using ancillary knowledge of sea-surface height to correct the estimated profiles. Such knowledge is not available a priori; indeed, its calculation is one motivation for acquiring salinity profiles. Satellite altimeter measurements may provide a sufficiently accurate approximation in the future. On the other hand, if salinity profiles can be estimated with sufficient accuracy by other means, the altimeter measurements can be used to refine the estimate of the temperature field or retained for use as a verification data set.

Emery and O'Brien [1978] found that using the mean salinity profile $\hat{S}(z) = <S(z)>$ gives more accurate estimates of geopotential height than does Stommel's method at latitudes higher than about 35°N in the Pacific. Our approach is to improve upon use of the mean salinity profile by exploiting correlations of salinity at a given depth z with other observables such as temperature at that depth, surface salinity, and latitude. The algorithm can be stated concisely as a generic regression equation:

$$\hat{S}(z) = <S(z)> + \sum_i a_i(z)(P_i - <P_i>)\,, \qquad (1)$$

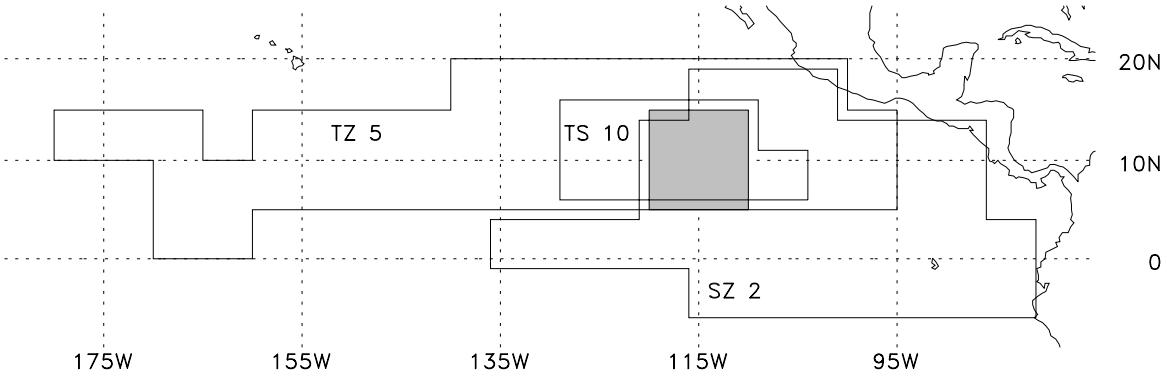

Figure 1. Region of this study (shaded square) in relation to the coastline and to the regions defined by *Emery and Dewar* [1982], whose area TS 10 is shifted 1° to the north and east and their area SZ 2 is shifted 1° to the south and west to remove ambiguity.

where angle brackets denote climatological averages, P_i represent the variables that are used as predictors, and the values of the coefficients a_i are derived from regressions for each depth z. Estimates are modifications of the climatological salinity profile by deviations of the observed predictors from their climatological means.

Temperature at the target depth is an obvious choice for a predictor. It provides information from the *T-S* relationship, which is valuable for accounting for adiabatic displacements. Surface salinity is anticipated to be a useful predictor in the mixed layer. It can be measured economically. Location is a no-cost predictor that potentially contains information about spatial variations. Seasonality might provide another no-cost predictor, but it was not used in this study.

We demonstrate the method in the context of a $10°\times 10°$ region in the eastern tropical Pacific Ocean (Figure 1). Characteristics of the region and the data obtained for it (Figures 2 and 3) are described in section 2, and in section 3, estimates from four variations of the method are compared to those obtained using the *T-S* method and the mean salinity profile. Some implications of use of this scheme are discussed in section 4, and section 5 discusses the merits of this approach.

2. Data

To demonstrate the algorithm, we apply it to estimation of salinity profiles for the $10°\times 10°$ region centered at 10°N latitude, 115°W longitude, immediately west of Clipperton Island. This choice was motivated partly by relevance to the program of Pan American Climate Studies and partly by the fact that this region appeared to offer substantial challenge for estimation of salinity.

Emery and Dewar [1982] classified the North Pacific and North Atlantic Oceans in terms of similarity of mean profiles $<T(z)>$, $<S(z)>$, and $\bar{S}[T(z)]$ in 5° latitude×longitude elements. As shown in Figure 1, the four 5° subregions of our area lie wholly within their area SZ 2, area TZ 5, and area TS 10. They estimated rms differences of about 8 cm from true geopotential heights of the sea surface relative to 500 dbar using $<S(z)>$ for area SZ 2 and more than 5 cm using the $\bar{S}[(T(z)]$ for area TS 10 with measured temperatures to estimate density. These values are about twice as large as counterparts over much of the central Pacific Ocean. *Wyrtki* [1974] shows a standard deviation of the geopotential height of the surface relative to 500 dbar of about 8 cm in this region. The errors found by *Emery and Dewar* [1982] imply a signal-to-noise ratio of order unity for calculation of variations of geopotential height anomaly by these methods. Indeed, for the southern half of our study region *Busalacchi et al.* [1994] also show 6 to 10 cm rms differences between sea-level variations from satellite altimeter and those derived from use of temperature profiles using a mean *T-S* relationship. Analyses of altimeter data from Geosat [*Maul et al.*, 1997] and TOPEX/POSEIDEN [*Wunsch and Stammer*, 1995] both indicate a zonal band of maximum sea-level variability with an rms amplitude of 10 to 12 cm, which suggests that perhaps a quarter of the sea-level variability arises from temperature and salinity variations at depths greater than 500 dbar.

There are several identifiable sources of variability of salinity in this region. The North Equatorial Countercurrent flows across the southern half of our chosen $10°\times 10°$ region, and at this longitude its surface velocity undergoes a nearly 100% annual modulation [*Reverdin et al.*, 1994]. The Intertropical Convergence Zone (ITCZ) of the atmosphere crosses the region, delivering heavy precipitation during the boreal summer. The observations of *Delcroix and Henin* [1991] suggest a maximum annual cycle of surface-salinity variation near 12°N with amplitude of 0.6 practical salinity units (psu) or more. Typically, during summer and autumn, tropical instability waves with 1000-km wavelength bring large variations of temperature, salinity, and currents to the southern part of the region [*Flament et al.*, 1996; *Hansen and Paul*, 1984]. Anticyclonic vortices of radius about 200 km, which appear to be generated by wind conditions near the coast of Central America, propagate through the center of

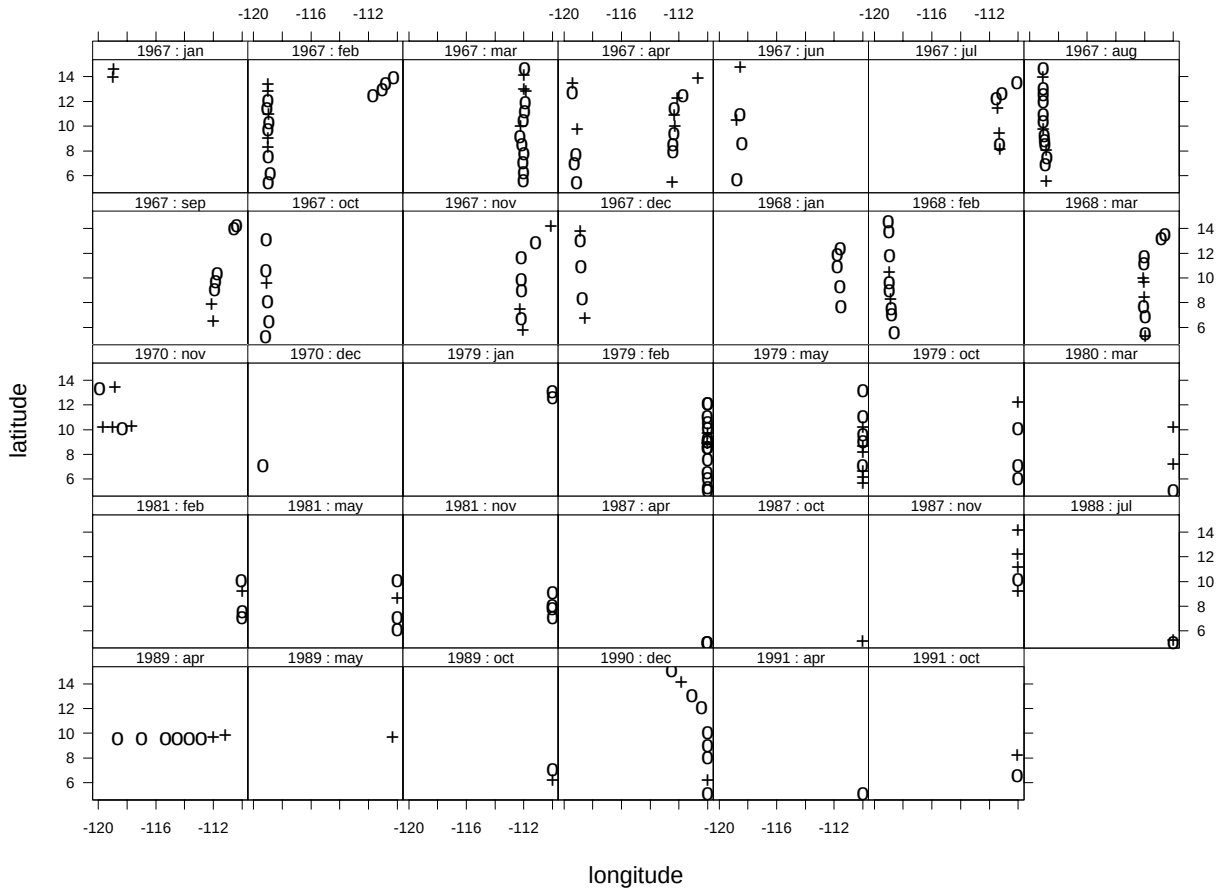

Figure 2. Time-space distribution of conductivity-temperature-depth (CTD) casts used in this study. Pluses indicate verification data; circles denote training data.

the area a few times a year [*Hansen and Maul*, 1991]. These vortices can have sea-level signatures in excess of 30 cm in association with a local doubling of thermocline depth. *Hansen and Maul* [1991] also found evidence that the *T-S* relationship for water within a vortex was distinct from that surrounding the ring. This difference is similar to that between area TS 10 of *Emery and Dewar* [1982] and their area TS 9, which lies east and north of area TS 10, extending to the coast of Central America where the vortices originate. This observation, as well as other chemical evidence suggests the presence of an alien water mass being transported in the vortices. Salinity variations are expected also in association with variable presence of Tropical Water [*Tsuchiya*, 1968] which is marked by a subsurface salinity maximum.

To develop the ideas presented in section 3, we obtained 291 measured conductivity-temperature-depth (CTD) profiles archived for the region by the National Oceanographic Data Center. Most of these profiles were collected for the Cooperative Effort Towards Understanding of the Oceanography of the Eastern Tropical Pacific Ocean (EASTROPAC) and the Equatorial Pacific Ocean Climate Study (EPOCS) programs and the marine mammal surveys of the National Marine Fisheries Service between 1967 and 1991. We rejected 74 of these profiles because they contained unrecoverable archival errors, were duplicates, or were highly redundant in time and location. All questionable profiles were checked against published cruise reports, data reports, or atlases for reasonableness in context. The spatial and temporal distribution of the 217 retained profiles is shown in Figure 2. Most of the profiles had data listed at exact 1-m intervals. Others, which had values for depths differing only slightly, were interpolated to these levels. Only data for the upper 500 m were used, because that range encompasses most XBT profiles and it facilitates comparisons with other works.

The salinity and temperature profiles and *T-S* curves for these data are shown in Figure 3. The salinity profiles reveal a large variability in the surface mixed layer with a range of nearly 2.5 psu. The haline mixed layer commonly reaches 30 m or more, indicating that surface salinity is a useful indicator of upper ocean salinity in this region. Also evident is the salinity maximum of the Tropical Water at about 100 m depth, although it is not as clearly expressed as in other parts of the tropical Pacific. Below a depth of about 200 m the scatter among the profiles becomes small. The temperature profiles exhibit much less variability in the surface mixed

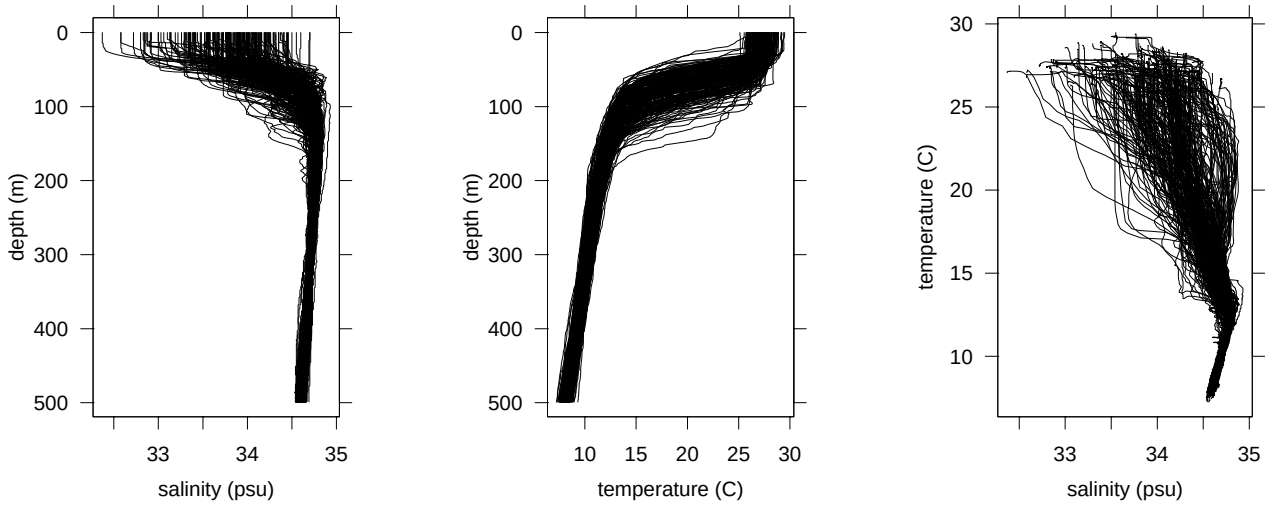

Figure 3. Profiles of (left) salinity-depth and (middle) temperature-depth and (right) temperature-salinity for the 217 CTD casts used in this study.

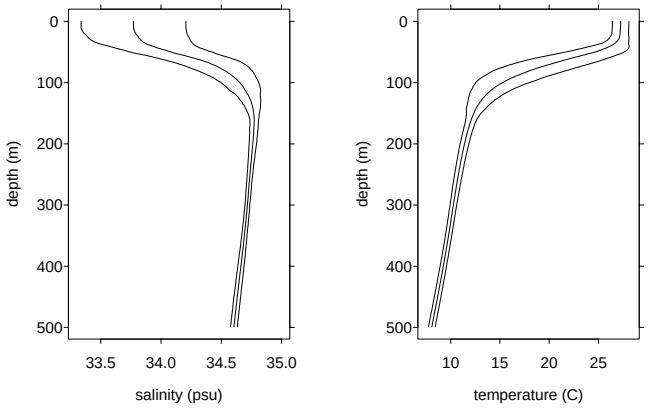

Figure 4. Mean values of (left) salinity and (right) temperature shown by thick curves for the 215 CTD casts used in this study, and standard deviations from the means shown by thin curves.

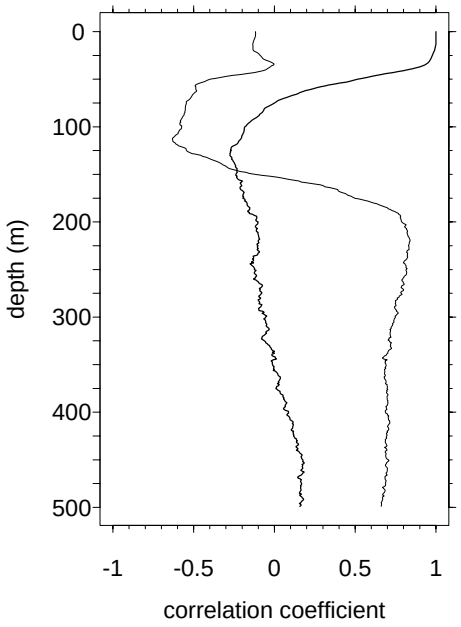

Figure 5. Correlation of surface salinity (thick curve) and local temperature (thin curve) with salinity at the specified depth.

layer and relatively little scatter below the thermocline. The *T-S* relationship is well defined for temperatures less than about 12°C but becomes increasingly ill defined from the bottom of the thermocline to the surface.

The mean profiles $<S(z)>$ and $<T(z)>$ are shown in Figure 4 together with their standard deviations. From these curves (Figure 4) we estimate that the contribution of salinity to the overall density stratification in the upper 100 m is about one fourth, and its contribution to variation of surface density is about equal to that of temperature. Correlation coefficients $\mathrm{cor}[S(z), T(z)]$ and $\mathrm{cor}[S(z), S(0)]$, which are central to the regression models discussed below, are shown in Figure 5. Correlation with temperature is negligible in the top 50 m, is small and negative between about 50 and 150 m, and is positive below 200 m. The reversal of sign of these correlations near 150 m reflects the presence of the salinity maximum of the Tropical Water, i.e., vertical displacements causing changes in S and T to have opposite signs. Correlation with surface salinity is strong in the upper 50 m, where correlation with temperature is poor, and negligible elsewhere. The complementary nature of these correlations suggests that their joint use should be advantageous. We omit discussion of the uncertainty of these correlations or those of the numerous coefficients used in the estimations

in favor of later showing the distribution of errors for the estimations of salinity and their propagation through the calculations of geopotential height.

The 217 temperature and salinity profiles were separated randomly using the S-Plus function `sample` [*Venables and Ripley*, 1994] into two sets, 145 profiles comprising the training data to be used for model fitting (indicated by circles in Figure 2) and 72 profiles for independent verification (crosses). Random selection was preferred to simply taking the first 2/3 of the casts as training data in order to avoid biasing the fit toward a generally cold sample.

3. Estimated Salinity Profiles From Six Methods

Salinity profiles were estimated for the upper 500 m using the *T-S* relationship, the mean salinity profile, and four variants of the regression procedure for the 72 profiles of the verification data set. The rms differences from the measured profiles were then computed and are shown in Figure 6.

T-S RELATIONSHIP. We first estimated the salinity profiles using the standard *T-S* method. Mean salinities for fixed values of temperature at 0.1°C intervals were evaluated for the training data. Then, for each temperature profile in the verification set, the salinity at each 1-m depth was estimated from the temperature at that depth by interpolating the *T-S* relationship from the training data:

$$\hat{S}(z) = \bar{S}[T(z)]\,; \tag{2}$$

This method is expected to serve poorly in the mixed layer where the *T-S* relationship is poorly defined. In near proximity to the surface it also suffers from the problem of too few data. (In the extreme case, near-surface values of a particular temperature profile being used to estimate salinity can exceed the highest temperatures observed in the past, so estimates must be based on extrapolations from the few highest values. We eliminated from consideration two profiles as excessively difficult in this regard.) The rms differences between the estimated and measured salinities for the verification profiles are labeled "*T-S* relationship" and appear as the rightmost profile near the surface and the left profile at 500 m in Figure 6, left. This method captures about half the variability at 200 m depth but only about one third at 500 m. Near the surface, errors slightly exceed the variability because of the difference between the training data and the verification data as well as the weakness of the *T-S* relationship in the near-surface region.

MEAN SALINITY. The second method we examine is estimation of salinity by its climatological mean:

$$\hat{S}(z) = <S(z)>\ . \tag{3}$$

The rms errors for this method are labeled "mean salinity" and appear as the left profile at the sea surface and the rightmost profile at 500 m in Figure 6, left. For this region the rms error is smaller than that achieved by use of the *T-S* method at most depths less than about 125 m and larger at depths greater than about 190 m. In the upper 50 m the errors are still large, slightly larger than the variability shown in Figure 4. The advantage of this method relative to the *T-S* method for computations of geopotential heights of the surface relative to 500 dbar in the North Pacific [*Emery and O'Brien*, 1978] results from the improvement in the near-surface waters outscoring the loss in the deeper waters. For the tropical and subtropical Pacific and for most of the North Atlantic, *Emery and Dewar* [1982] found the *T-S* method to give smaller errors.

TEMPERATURE. The complementarity of depths at which the *T-S* and climatological mean methods perform best suggests merger of these methods, using observed temperature to improve upon the climatological mean salinity in a regression model:

$$\hat{S}(z) = <S(z)> + a_T(z)[T(z) - <T(z)>]\,. \tag{4}$$

We have found no mention of this method in the oceanographic literature. This model and those discussed below were fitted to the training data using the S-Plus function `lm` [*Venables and Ripley*, 1994]. Although the model was fitted independently at each 1-m interval, the coefficients varied smoothly with depth. The rms errors, labeled "temperature" in the Figure 6, left, show that this approach realizes the best of the two previous methods; in the upper 50 m it matches the skill arising from use of the mean profile, and at depths exceeding about 180 m it matches results from use of the *T-S* method. Between 50 and 130 m it exceeds the skill of both these methods, and in the depth interval 130 to 180 m all methods are equivalent.

SURFACE SALINITY. We turn now to the issue of using measurements of surface salinity to capture some of the variability that characterizes the upper several tens of meters. First, we consider their use in the absence of an observed temperature profile. At each depth z a regression equation establishes how deviations of the observed surface salinity from its mean modify the estimates based on the mean salinity profile:

$$\hat{S}(z) = <S(z)> + a_S(z)[S(0) - <S(0)>]\,. \tag{5}$$

Owing to the strong correlation of $S(z)$ with $S(0)$ in the upper 50 m of the water column, the rms estimation error, labeled "surface salinity" in Figure 6, right, is reduced to 0.2 psu or less in the top 40 m. Within the top 25 m the estimation error is less than 0.1 psu. Deeper than about 60 m surface salinity provides no information, the regression coefficient $a_S(z)$ is essentially zero, and the "surface salinity" curve of Figure 6, right, becomes coincident with the "mean salinity" curve of Figure 6, left.

BOTH. It is straightforward to include deviations of both surface salinity and the temperature profile from their means to estimate deviations of salinity:

$$\begin{aligned}\hat{S}(z) = <S(z)> \quad &+ \quad a_T(z)[T(z) - <T(z)>] \\ &+ \quad a_S(z)[S(0) - <S(0)>]\,.\end{aligned} \tag{6}$$

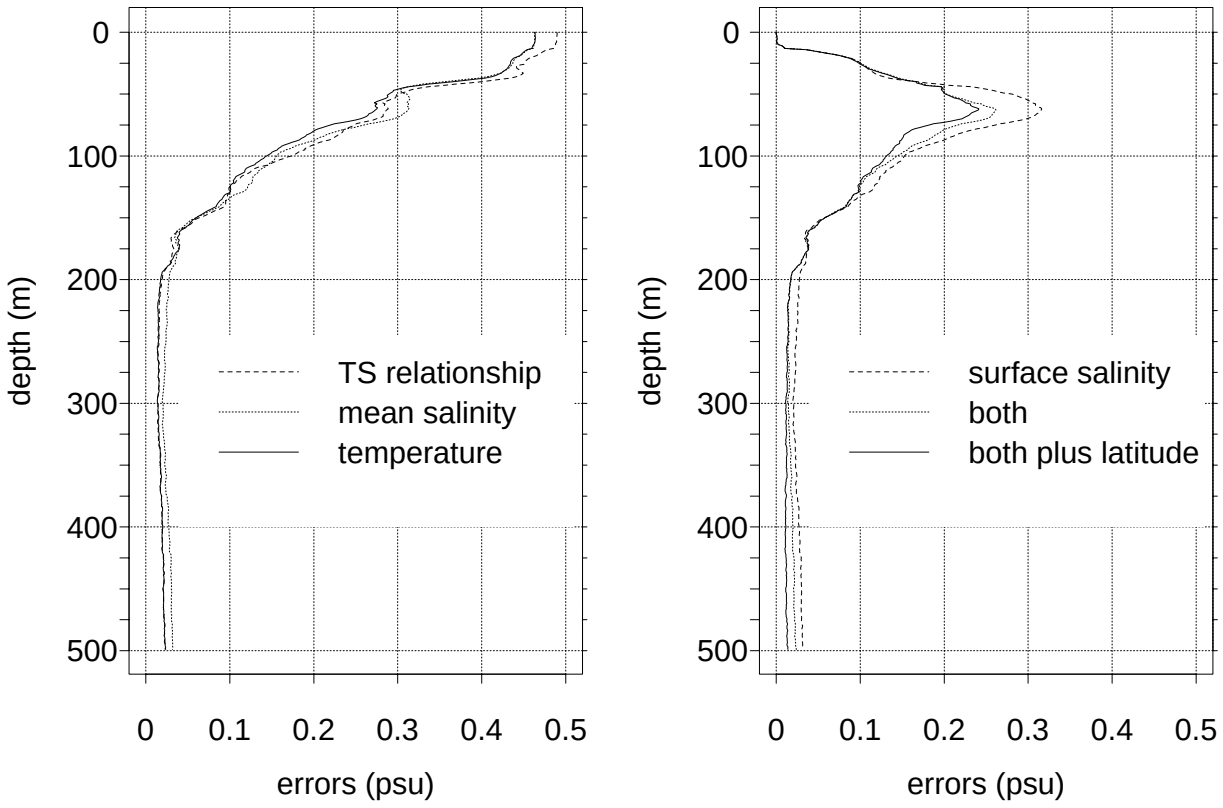

Figure 6. Root-mean-square errors for various methods of estimating the salinity profiles of the verification data. (left) Errors for the *T-S* relationship, mean salinity profile, and regression on temperature. (right) Errors for regression on surface salinity; both surface salinity and temperature; and surface salinity, temperature, and latitude.

The values of the coefficients a_T and a_S are not the same as those for (4) and (5); they must be determined by fitting (6) to the training data. However, at depths where surface salinity carries no information about the subsurface salinity, it turns out that $a_S(z) \approx 0$ and $a_T(z)$ is the same as that found for (4). The curve labeled "both" in Figure 6, right, indicates that near the surface this extension yields no improvement over use of surface salinity, but it further reduces errors in the thermocline where salinity has modest but helpful correlation with temperature. At all depths greater than about 180 m its error profile overlays those of the two methods in Figure 6, left, that use temperature-profile data.

BOTH PLUS LATITUDE. All of the methods we have described are expected to do best in application to a homogeneous water mass. However, for reliable statistics, data must be drawn from a sizeable region, e.g., our $10^\circ \times 10^\circ$ region, over which horizontal gradients of water properties may contribute significantly to the variances about the mean profiles. To test the possibility of capturing part of this variability, we added latitude ϕ to the other predictors, because the climatological structure in the tropical oceans is primarily zonal:

$$\begin{aligned} \hat{S}(z) = <S(z)> \quad &+ \quad a_T(z)[T(z) - <T(z)>] \\ &+ \quad a_S(z)[S(0) - <S(0)>] \\ &+ \quad a_\phi(z)[\phi - <\phi>] \, . \end{aligned} \tag{7}$$

Use of latitude was surprisingly beneficial, yielding (leftmost curve in Figure 6, right) some further reduction of errors in the troublesome interval from 50 to 125 m and also at all depths greater than about 200 m. At 500 m the error relative to either the conventional *T-S* method or our mean-salinity-plus-temperature method, with or without a surface-salinity measurement, is diminished by nearly half, to about 0.012 psu. In the upper 50 m the errors are nearly coincident with those from the other methods using surface salinity. As before, the coefficients were smooth functions of z with (7) reducing to the simpler models when predictors offer no information. Note that at each level z there are four coefficients ($a_T(z)$, $a_S(z)$, $a_\phi(z)$, and an intercept) determined by data from the 145 training casts, so there are many more data than unknowns, allowing the continuity of the data to be manifest as continuity of coefficients. (We also added longitude to this set of predictors and found results that were indistinguishable from those obtained using (7)).

We have presented results from six methods of estimating salinity profiles, including the two conventional procedures using the mean salinity and the regional *T-S* relationship. The curves shown in Figure 6 sort themselves into three classes in the near surface and into three different classes in deep waters, while all six are nearly indistinguishable at depths near 150 m. In the near-surface levels the largest

errors are associated with the *T-S* method, but mean salinity, with or without the addition of temperature data, is only slightly better. Only the use of salinity as a predictor substantially reduced the rms estimation error. Addition of surface-salinity information to the climatological profile reduces the estimation error to 0.1 psu or less in the upper 25 m and outperforms the *T-S* method to about 50 m.

At depths of 50 to 120 m, inclusion of temperature information by regression is more beneficial than by the *T-S* relationship, and at depths greater than 180 m all of the methods using temperature provide equivalent results, reducing the errors to 0.025 psu or less. Surface salinity provides no improvement at depths exceeding about 70 m. Finally, inclusion of latitude gives further improvement in the lower part of the thermocline and deeper than 250 m, yielding the smallest errors at nearly all depths. Below about 400 m the error is then reduced to half that obtained with the best of the methods not using latitude. The model (7) performs best in all depth ranges. While it is better in principle to use the simpler models at depths where some predictors carry no information, this was not an issue here, as the results were identical when the uninformative predictors were retained.

4. Discussion

We have examined the quality of replication achieved for each of the 72 profiles of the verification set. We find that when surface salinity is much below average, the salinity profiles are quite realistic, capturing barrier layers when they are present. Mesoscale instability waves and warm-core rings were major contributors to the rms error. We have also calculated the rms error of geopotential height relative to 500 dbar for each the methods described for the verification data.

4.1. Individual Profiles

Interest has grown in the occurrence of barrier layers, i.e., density-stratified layers defined by the presence of a halocline in the near-surface isothermal layer. Such structure was described by *Defant* [1981] in observations of the tropical Atlantic from the *Meteor* cruise of 1925-1927. Recently, *Sprintall and Tomczak* [1992] have offered evidence that the occurrence of barrier layers is quite general in the global tropics. Suggested causal mechanisms vary by region, but the common denominator seems to be a local excess of precipitation and/or river discharge over evaporation. Barrier layers cannot be recovered when estimating salinity profiles with the conventional *T-S* method, because the functional forms of the salinity profiles are essentially different from those of the temperature profiles. *Sprintall and Tomczak* [1992] showed that some barrier-layer information is implied even in the climatological salinity profiles. All of the regression methods therefore have the capability of producing barrier layers. This capability is enhanced by the use of surface-salinity measurements.

To illustrate the ability of the new algorithm (7) to replicate individual salinity profiles, all 72 observed and estimated salinity profiles of the verification data set are displayed in Figure 7; the associated temperature profiles are shown in Figure 8. In general, the quality of the replications is much better than might have been expected from Figure 3. Moreover, the method seems to handle situations with anomalously low surface salinity especially well. An outstanding example is from cast 30, which was made during an EASTROPAC cruise of *R/V David Starr Jordan* in late October 1967. The low surface salinity reflects that this location had been under the ITCZ, experiencing heavy precipitation during the preceding several months. Replication of the CTD salinity profile is excellent, showing a strong halocline from the surface to nearly 75 m depth. The corresponding temperature profile reveals a temperature inversion sustained by the strength of the halocline. This situation might be called a "superbarrier layer." In this situation, vertical mixing is likely to be excessive in a numerical circulation model in which salinity is not well characterized. Evidence of other superbarrier layers can be seen in casts 5, 14, and 25. Other barrier layers can be discerned in casts 21, 23, and 72. All of these obvious barrier layers except those in casts 5 and 14 occur at times and locations where influences of both the ITCZ and the North Equatorial Countercurrent are expected.

Profiles with large positive departures of surface salinity from the mean are not handled as well. Examples are profiles 27 and 46. Surface salinity in the measured profiles is almost as high as is expected in the salinity maximum of the Tropical Water, and large variability with evidence of interleaving layers can be seen between 100 and 200 m depth. Temperature of the surface waters is nearly normal, the thermoclines are deep, and, especially in 27, there is an unusual amount of stratification above the main thermocline. Near the sea surface the estimated salinity profile is well controlled by surface salinity, but at depths where the correlations with surface salinity become small (Figure 5) the unusually deep thermocline and reversion toward climatology contribute to a fictitious salinity minimum between about 50 and 120 m.

Neither the *T-S* nor the mean-salinity method will to do as well for large positive surface-salinity anomalies. The *T-S*-linear method proposed by *Vossepoel et al.* [1999] is likely to be very sensitive to the definition of the bottom of the thermal mixed layer. With their criterion (0.5°C temperature change from the sea surface) the fictitious salinity minima will be shallower and stronger than those we obtained. Reducing them using sea-surface-height measurements probably would force compensating salinity mismatches at deeper levels. Only closely spaced measurements are likely to reveal the complicated structures seen below 100 m in these and a few other casts. These profiles were observed in the seasons and locations wherein tropical instability waves usually appear except during years of El Niño [*Philander et al.*, 1985]. Neither 1967 nor 1970 was a recognized El Niño year, so it appears likely that these unusual profiles of both salinity and temperature were associated with tropical instability waves. As such, they are highly transient phenomena outside the aspiration of present data assimilation efforts and

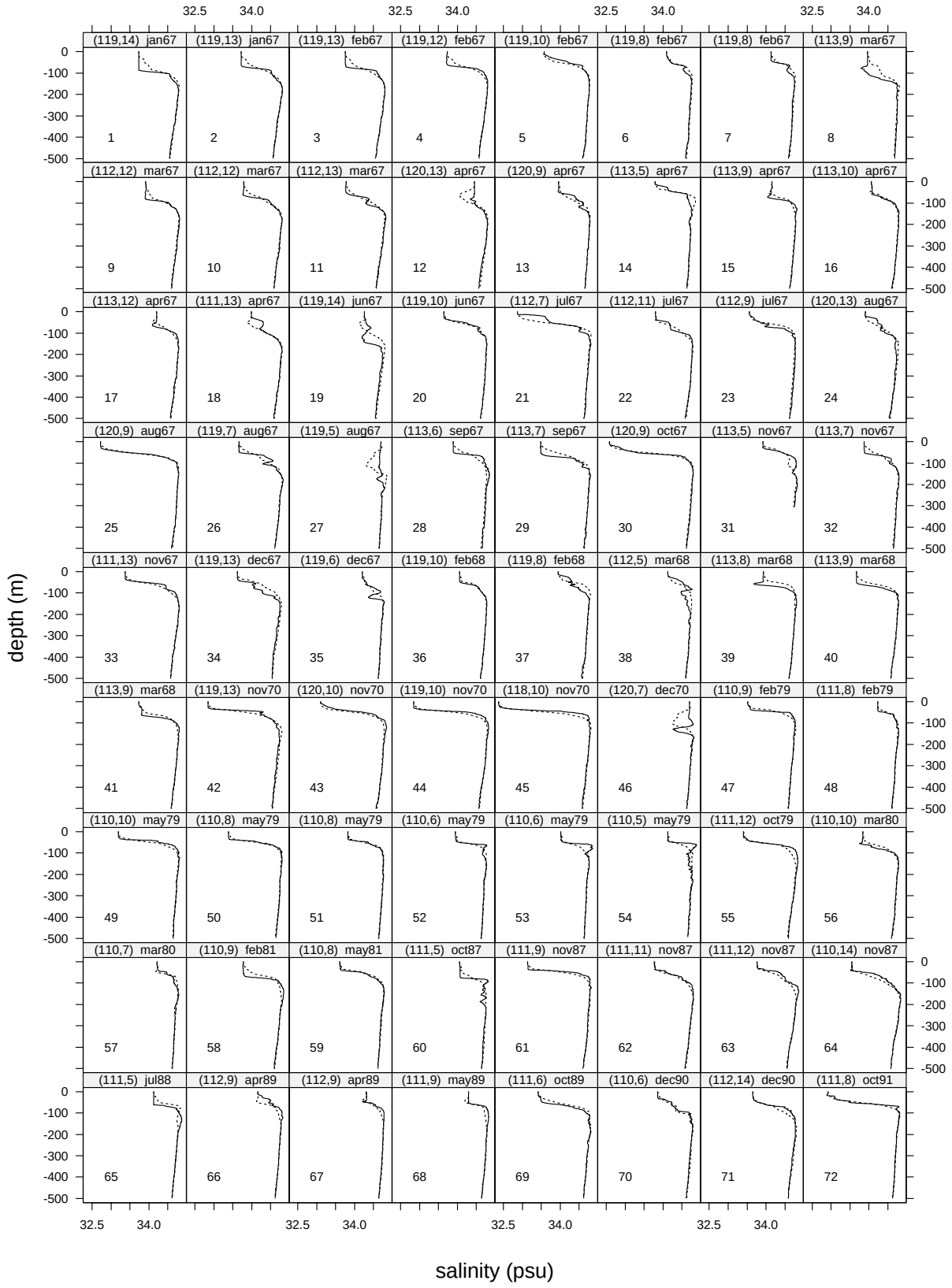

Figure 7. Estimated (dotted curves) and observed (solid curves) profiles of salinity for the 72 casts that were not used in establishing statistical relationships. Labels give longitude (°W) and latitude (°N) rounded down to the nearest integer, as well as month and year.

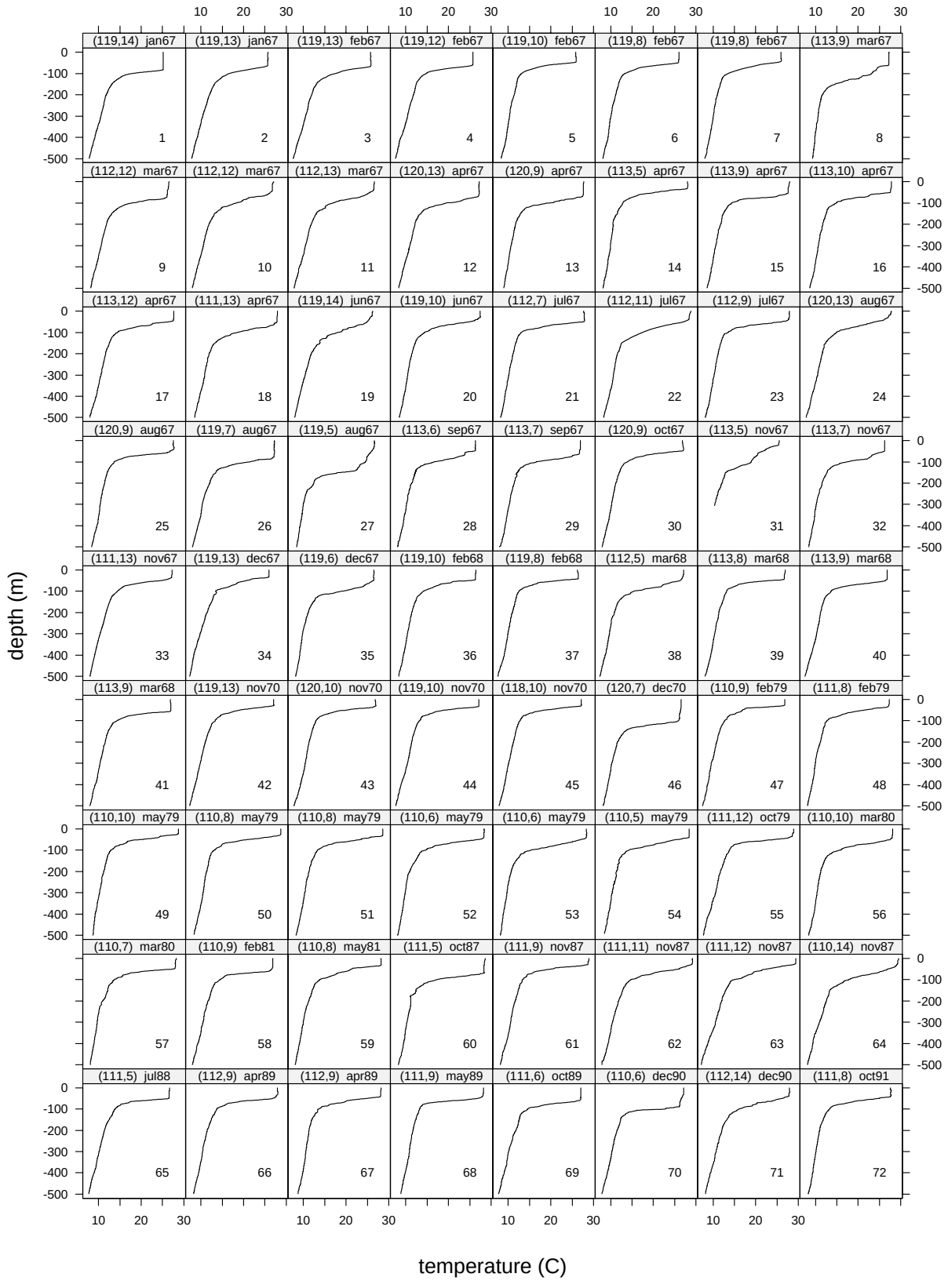

Figure 8. Observed profiles of temperature that were used in estimating the salinity profiles shown in Figure 7.

of little relevance for predicting climate.

For cast 1 and some near it in sequence, surface salinity is nearly normal and the measured depths of both the thermocline and the halocline are relatively deep. The mixed-layer temperature is nearly 2°C below average, probably reflecting the winter phase of the annual cycle, which we have not tried to represent in the estimation model. This situation produces positive estimation errors at depths where correlation with surface salinity becomes weak. The anomalously deep thermocline and halocline, together with the season and location, lead us to conjecture that this profile was measured in a mesoscale vortex of the kind described by *Hansen and Maul* [1991]. If this conjecture is correct, again, none of the mean-salinity, *T-S*, or *T-S*-linear methods can be expected to serve better,as this is a water mass alien to the region contained in a mesoscale distortion.

These problem profiles and a few others similar to them exhibit the largest mismatches to be seen in Figure 7. They are major contributors to the maximum in residual variance shown near 60-m depth in Figure 6. If these profiles are associated with energetic mesoscale processes as has been suggested, they are largely irrelevant for assimilation in models for which the objective is simulation of large-scale, low-frequency processes. Occurrences of these mesoscale phenomena are revealed in satellite observations of sea-surface temperature (instability waves) and altimeter (vortices) measurements. Profile estimates in the presence of these phenomena can therefore be screened from the analyses if they are thought to create problems. Although it reduces the number of observations available for the analyses, such screening offers the benefit of of reducing the rms salinity errors in the thermocline while removing features irrelevant to the analyses from the data.

4.2. Estimates of Geopotential Height

To evaluate the merits of the several methods described for estimation of salinity profiles in calculation of geopotential heights, we calculated the geopotential-height anomaly of the surface relative to 500 dbar for 69 casts of the verification data set using the estimated salinities with measured temperatures to determine specific volume and subtracted the "true" geopotential heights calculated from measured salinities and temperatures. (Three of the 72 verification casts did not reach 500-m depth and two additional casts were excluded from the calculation using the *T-S* method.) The differences are summarized in Figure 9.

For methods not using surface salinity the differences are skewed. The skewness is almost entirely removed by use of surface salinity in the estimation of the salinity profiles. The median error is less than 1 cm for all methods, but when surface salinity is used, they are reduced to less than 2 mm. The largest rms errors resulted from use of the *T-S* method, but these are only 2.23 cm, surprisingly small compared to the roughly 5 cm errors found by *Emery and Dewar* [1982] using this method. Even more surprising, use of the mean salinity yielded an rms error of only 1.84 cm, less than a

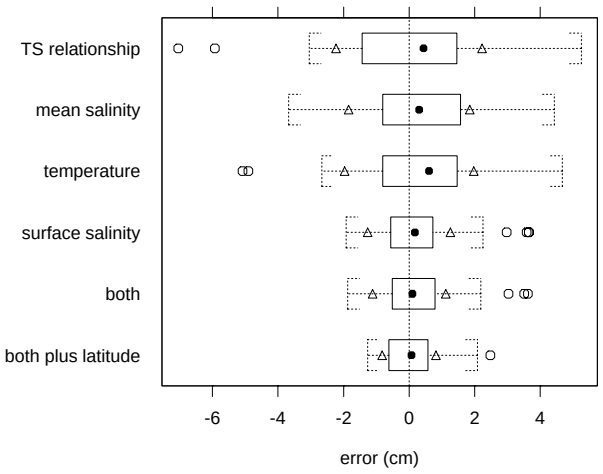

Figure 9. Errors in estimates of geopotential height resulting from the six methods of estimating salinity. Solid circles indicate median error for 69 casts (67 casts for *T-S* relationship), solid box indicates interquartile range, open circles indicate outliers, whiskers extend to the nearest value not beyond 1.5 times the interquartile range, and triangles indicate root-mean-square error range.

quarter of the 6 to 10 cm errors reported by *Emery and Dewar* [1982]. We traced these differences primarily to salinities as much as 0.6 psu higher than ours at depths less than 150 m in the $<S(z)>$ profile or at temperatures from about 14°C to 26°C in the *T-S* relationship. These differences do not seem to arise from the selection of region, because their SZ and TS regions are quite different (Figure 1). Because we do not have detailed knowledge of their (mostly bottle) data set, we did not pursue the issue further. Defects in their data undoubtedly contribute to these differences, but it also appears that the smoothing procedure adopted to reduce extreme variability in the profiles is likely to increase salinity at depths above the Tropical Water. Our estimation of salinity using an observed temperature profile with the mean-salinity profile yielded errors of geopotential height that, in general, have a little tighter distribution but, owing to two outliers, have an rms value (1.97 cm) that is slightly larger that that from using the mean salinity alone but still smaller than that from the *T-S* method.

Use of surface salinity with mean salinity further narrows the range of geopotential-height errors and reduces the rms error to 1.26 cm. Addition of temperature profile and latitude data progressively reduces the rms error to 0.82 cm and the median value to near zero. These results are very comparable to those shown by *Vossepoel et al.* [1999], with or without use of ancillary sea-surface height information, for the part of their study region that overlaps ours.

Over most of the equatorial Pacific the rms surface-height variation is 6 to 8 cm [*Wunsch and Stammer*, 1995]. In large parts of the subtropics, especially in the Atlantic, it is less than 4 cm. In the region that we have considered, the variations are significantly larger, but even here, use of the al-

gorithm presented with an ancillary measurement of surface salinity can provide geopotential heights with errors due to estimation of salinity of less than 1 cm. Without surface salinity it is possible to estimate geopotential-height anomalies from temperature profiles and readily available location information with an rms error of less than 2 cm. This is in accord with findings of previous investigators, who have obtained apparently reasonable results with diverse incorporations of surface salinity, or none at all.

Profiles to be used for assimilation into models to be used for analyses and prediction of large-scale, low-frequency phenomena are contaminated by high-frequency geophysical variations that introduce about 1 cm random noise into geopotential-height calculations [*Hayes*, 1982]. In the tropical Pacific, variations of the density field deeper than 500 m are estimated to contribute 5 to 15% of the geopotential-height variation of the sea surface [*Busalacchi et al.*, 1994]. Temperature-measurement errors from moorings are expected to be uncorrelated in the vertical, while those from XBTs may contain profile biases. In the latter case the change in sign of $\mathrm{cor}[S(z), T(z)]$ (Figure 5) will tend to reduce the effect of temperature-measurement errors in geopotential-height calculations. Temporal stability of sea-surface-salinity measurements from buoys is complicated by biofouling. The impact of this kind of measurement error on geopotential-height calculations for our test region, and likely over much larger regions, is limited by the depth range over which $\mathrm{cor}[S(z), S(0)]$ is significant (Figure 5). Thus in our area the effect of this measurement error on geopotential-height calculations is an order of magnitude smaller than that of the same error applied over a thickness of 500 m. The error of the means and covariances derived from an adequate sample with modern CTD equipment seems inconsequential. The important figure of merit is the regional signal-to-noise ratio of the surface salinity measurement.

5. Conclusion

We have described a hierarchy of methods for estimating salinity profiles in the upper ocean using climatological data with or without contemporary observations of surface salinity. The skills of the various methods were demonstrated for a region selected for its apparent difficulty. Sea-surface salinity provides additional information relevant to the part of the salinity profile where the uncertainty otherwise is greatest. It is also a relatively easy measurement to obtain and offers potential for large-scale mapping via remote sensing in the future. With the addition of sea-surface salinity to the estimation of salinity profiles, the rms error in calculation of the geopotential-height anomaly of the sea surface relative to 500 dbar is reduced to less than 1 cm. This error might be reduced further by judicious exclusion of profiles influenced by processes irrelevant to the objectives of the analysis.

Estimates of salinity profiles that exploit measurements of sea-surface salinity, when assimilated into numerical models of the ocean, can be expected to lead to other improvements that may equal in value the improvement to geopotential heights. In particular, in the modest number of examples that we have examined, our estimation algorithm appears to perform especially well in the case of anomalously fresh surface water, a situation frequently associated with the occurrence of barrier layers in the thermal mixed layer. Identification of barrier layers allows refinements of upper-ocean heat-budget studies such as that of *Swenson and Hansen* [1999]. Assimilation of surface-salinity observations into ocean analyses therefore can improve modeling of turbulent exchange processes in the upper ocean. Improving the structure of the Ekman flow will make the currents from the analyses much more valuable to a host of secondary users. For example, improved estimates of salinity and associated improvements in estimated currents can support computations of freshwater budgets and transports of potentially great value for a broad range of climate applications. For instance, *Rahmstorf* [1996] describes the importance of freshwater transport for meridional heat transport in the Atlantic Ocean.

Even without additional measurements of surface salinity the formalism presented here for estimation of salinity profiles offers some advantage over previous methods. For a region of the eastern Pacific Ocean containing diverse sources of variability, geopotential-height anomalies of the sea surface relative to 500 dbar can be calculated with an rms error of about 2 cm using only the climatological data. Results from use of climatological salinity-profile data were slightly better than those obtained using the traditional *T-S* method and have the added advantage of being capable of retaining at least part of barrier-layer structures where these are a common feature. We expect that use of salinity with temperature profile and location data will reduce further the rms error of geopotential heights by about 0.3 cm in this region. Including salinity in estimations of stratification may be of value in applications that heretofore, by necessity, have not considered salinity at all, such as mixed-layer heat-budget studies in which the mixed layer has been defined in terms of a bulk temperature difference.

Extensive use of (7) in support of ocean analyses based on assimilation of observations into circulation models will require enhancement of surface-salinity observations and compilation of the climatological means. Application of (4) to regional analyses for which the *T-S* method has been used heretofore is obvious and straightforward and can be improved by including location data.

We have obtained good results for a region that we perceived to be problematic. An appropriate next step is to test the method for regions with other kinds of problems or important features. One example is the western tropical Pacific, where barrier layers appear to be of particular importance and where major changes of salinity occur with ENSO events. Another is the Pacific Ocean north of about 35°N.

Acknowledgments. This work was supported partly by the Pan American Climate Studies, and partly by the Atlantic Oceanographic and Meteorological Laboratory of the National Oceanic and Atmospheric Administration. Its presentation has benefited

from helpful discussions with S. Garzoli, R. Molinari, M. Swenson, and D. Mayer.

References

Acero-Shertzer, C. E., D. V. Hansen, and M. S. Swenson, Evaluation and diagnosis of surface currents in the National Centers for Environmental Prediction's ocean analyses, *J. Geophys. Res.*, *102*, 21,037–21,048, 1997.

Busalacchi, A. J., M. J. McPhaden, and J. Picaut, Variability in equatorial Pacific sea surface topography during the verification phase of the TOPEX/POSEIDON mission, *J. Geophys. Res.*, *99*, 24,725–24,738, 1994.

Carton, J. A., and E. C. Hackert, Data assimilation applied to the temperature and circulation in the tropical Atlantic, 1983–84, *J. Phys. Oceanogr.*, *20*, 1150–1165, 1990.

Chassignet, E. P., L. T. Smith, R. Bleck, and F. O. Bryan, A model comparison: Numerical simulations of the North and Equatorial Atlantic oceanic circulation in depth and isopycnic coordinates, *J. Phys. Oceanogr.*, *26*, 1849–1867, 1996.

Cooper, N. S., The effect of salinity on tropical ocean models, *J. Phys. Oceanogr.*, *18*, 697–707, 1988.

Defant, A., *Stratification and Circulation of the Atlantic Ocean: The Troposphere*, Amerind Publishing Company, New Delhi, 1981.

Delcroix, T., and C. Henin, Seasonal and interannual variations of sea surface salinity in the tropical Pacific Ocean, *J. Geophys. Res.*, *96*, 22,135–22,150, 1991.

Delcroix, T., C. Henin, V. Porte, and P. Arkin, Precipitation and sea-surface salinity in the tropical Pacific Ocean, *Deep-Sea Res., Part 1*, *43*, 1123–1141, 1996.

Donguy, J. R., G. Eldin, and K. Wyrtki, Sealevel and dynamic topography in the western Pacific during 1982-1983 El Nino, *Trop. Ocean-Atmos. Newslett.*, *36*, 1–3, 1986.

Emery, W. J., and J. S. Dewar, Mean temperature-salinity, salinity-depth, and temperature-depth curves for the North Atlantic and the North Pacific, *Prog. Oceanog.*, *11*, 219–305, 1982.

Emery, W. J., and A. O'Brien, Inferring salinity from temperature or depth for dynamic height calculations in the North Pacific, *Atmosphere-Ocean*, *16*, 348–366, 1978.

Flament, P. J., S. C. Kennan, R. A. Knox, P. P. Niiler, and R. L. Bernstein, The three-dimensional structure of an upper ocean vortex in the tropical Pacific Ocean, *Nature*, *383*, 610–613, 1996.

Flierl, G. R., Correcting expendable bathythermograph (XBT) data for salinity effects to compute dynamic heights in Gulf Stream rings, *Deep-Sea Res.*, *25*, 129–134, 1978.

Hansen, D. V., and G. A. Maul, Anticyclonic current rings in the eastern tropical Pacific Ocean, *J. Geophys. Res.*, *96*, 6965–6979, 1991.

Hansen, D. V., and C. A. Paul, Genesis and effects of long waves in the equatorial Pacific, *J. Geophys. Res.*, *89*, 10,431–10,440, 1984.

Hayes, S. P., A comparison of geostrophic and measured velocities in the equatorial undercurrent, *J. Marine Res.*, *40*, 219–229, 1982.

Hénin, C., and J. Grelet, A merchant ship thermo-salinograph network in the Pacific Ocean, *Deep-Sea Res.*, *43*, 1833–1855, 1996.

Ji, M., and A. Leetmaa, Impact of data assimilation on ocean initialization and El Niño prediction, *Mon. Wea. Rev.*, *125*, 742–753, 1997.

Ji, M., A. Leetmaa, and J. Derber, An ocean analysis system for climate studies, *Mon. Wea. Rev.*, *123*, 460–481, 1995.

Kessler, W. S., and B. A. Taft, Dynamic heights and zonal geostrophic transports in the central tropical Pacific during 1979–1984, *J. Phys. Oceanogr.*, *17*, 97–122, 1987.

Lagerloef, G. S. E., C. T. Swift, and D. M. Le Vine, Sea surface salinity: The next remote sensing challenge, *Oceanography*, *8*, 44–50, 1995.

Lucas, R., and E. Lindstrom, The mixed layer of the western equatorial Pacific Ocean, *J. Geophys. Res.*, *96*, 3343–3357, 1991.

Maul, G. A., M. H. Bushnell, N. J. Bravo, and D. V. Hansen, Observed sea surface height and modeled dynamic height anomaly departures in the tropical Pacific Ocean: 1986-1989, *Oceanol. Acta*, *20*, 569–584, 1997.

Miller, J. L., M. A. Goodberlet, and J. B. Zaitzeff, Airborne salinity mapper makes debut in coastal zone, *EOS Trans. Am. Geophys. Union*, *79*, 173, 176–177, 1998.

Philander, G., D. Halpern, D. Hansen, R. Legeckis, L. Miller, C. Paul, R. Watts, R. Weisberg, and M. Wimbush, Long waves in the equatorial Pacific, *EOS Trans. Am. Geophys. Union*, *66*, 154, 1985.

Rahmstorf, S., On the freshwater forcing and transport of the Atlantic thermohaline circulation, *Clim. Dyn.*, *12*, 799–811, 1996.

Reason, C. J. C., On the effect of ENSO precipition anomalies in a global ocean GCM, *Clim. Dyn.*, *8*, 39–47, 1992.

Reverdin, G., C. Frankignoul, , E. Kestenare, and M. J. McPhaden, Seasonal variability in the surface currents of the equatorial Pacific, *J. Geophys. Res.*, *99*, 20,323–20,344, 1994.

Reynolds, R. W., M. Ji, and A. Leetmaa, Use of salinity to improve ocean modeling, *Phys. Chem. Earth*, *23*, 543–553, 1998.

Roemmich, D., M. Morris, W.R.Young, and J.R.Donguy, Fresh equatorial jets, *J. Phys. Oceanogr.*, *24*, 540–558, 1994.

Schneider, N., and P. Müller, Sensitivity of the surface equatorial ocean to the parameterization of vertical mixing, *J. Phys. Oceanogr.*, *24*, 1623–1640, 1994.

Sprintall, J., and M. Tomczak, Evidence of the barrier layer in the surface layer of the tropics, *J. Geophys. Res.*, *97*, 7305–7316, 1992.

Stommel, H., Note on the use of the T-S correlation for dynamic height anomaly calculations, *J. Marine Res.*, *VI*, 85–92, 1947.

Swenson, M., and D. Hansen, Tropical Pacific Ocean mixed-layer heat budget: The Pacific cold tongue., *J. Phys. Oceanogr.*, *29*, 69–81, 1999.

Tsuchiya, M., *Upper Waters of the Intertropical Pacific Ocean*, The Johns Hopkins Press, Baltimore, 1968.

Venables, W. N., and B. D. Ripley, *Modern Applied Statistics with S-Plus*, Springer-Verlag, New York, 1994.

Vossepoel, F. C., R. W. Reynolds, and L. Miller, Use of sea level observations to estimate salinity variability in the tropical Pacific, *J. Atmos. Ocean. Technol.*, 1999, in press.

Wijffels, S. E., R. W. Schmitt, H. L. Bryden, and A. Stigebrandt, Transport of freshwater by the oceans, *J. Phys. Oceanogr.*, *22*, 155–162, 1992.

Wunsch, C., and D. Stammer, The global frequency-wavenumber spectrum of oceanic variability estimated from TOPEX/POSEIDON altimetric measurements, *J. Geophys. Res.*, *100*, 24,895–24,910, 1995.

Wyrtki, K., The dynamic topography of the Pacific Ocean and its fluctuations, *Rep. HIG-74-5* Hawaii Inst. of Geophys., University of Hawaii, Honolulu, 1974.

D. V. Hansen, Atlantic Oceanographic and Meteorological Laboratory, 4301 Rickenbacker Causeway, Miami, FL 33149. (hansen@aoml.noaa.gov)

W. C. Thacker, Atlantic Oceanographic and Meteorological Laboratory, 4301 Rickenbacker Causeway, Miami, FL 33149. (thacker@aoml.noaa.gov)